Three-dimensional model system for baroclinic estuarine dynamics and suspended sediment transport in a mesotidal estuary

L. Cancino, R. Neves

Department of Mechanical Engineering, Instituto Superior Técnico, Av. Rovisco Pais, P-1096 Lisboa, Portugal

Abstract

A coupled 3D-baroclinic hydrodynamic and cohesive sediment transport model applied to the Western Scheldt estuary is presented. The use of the two-fold sigma coordinate considerably improves the results on intertidal zones. The simulations provide an insight into the effetcs of stratification and its tidal asymmetry into the sediment transport. The calculated density current show an intensity two order of magnitute lower than the residual barotropic currents. The turbidity maximum is not directly associate to the density currents but mainly with the variation of estuarine horizontal area. Numerical results are compared with field measurements at several locations.

1 Introduction

Estuaries are transitional areas that trap significant quantities of particulate and dissolved matter, originating a wide variety of biogeochemical processes and thus acting as filters between the land and the sea. The filtering efficiency for particulate matter is strongly conditioned by the general circulation pattern, the flocculation and sedimentation processes and the activities of filter-feeders in the bottom and in the water column. This filtering role makes them crucial systems for the study of global change phenomena and subject to particularly strong human influence. Among the many problems related to antropogenic activities in estuarine environments those related to sediment dynamics assume great importance for direct monitoring because of their implication in morphological evolution due to engineering activities and urban development, and also indirectly due to water quality problems.

Influence of the sediments in an estuary is not limited to its role on material transport and deposition. Dense cohesive sediment suspensions (cohesive sediments are particles smaller than 63mμ), inhibiting light penetration, affect photosynthesis causing a decrease in phytoplankton production and consequently conditioning the whole food chain.

Mathematical modelling has been extensively applied since it is an important contribution for the understanding and prediction of estuarine problems allowing the establishment of effective monitoring programmes, the prediction of how vulnerable to contamination can certain areas be and rational contingency planning.

2 Main Features of the Western Scheldt Estuary

The Western Scheldt estuary, located on the southwest Netherlands, west Belgium, is constituted by the confluence of several rivers. The total drainage basin has an extent of 21600 km^2 covering one of the most heavily populated regions of Europe.

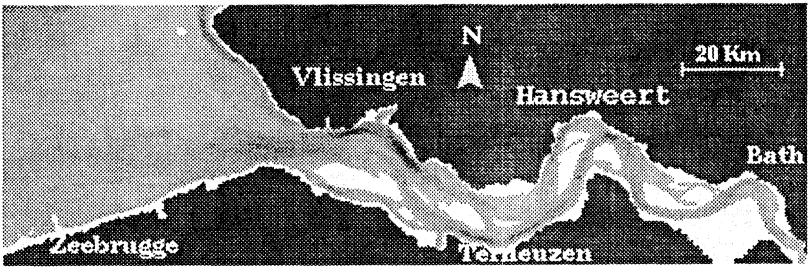

Figure 1: Bathymetry of the Western Scheldt estuary. Lighter grey indicates intertidal areas.

It is a large and narrow mesotidal coastal plain estuary with strong curvature. The upper estuary is characterized by a single and narrow channel with tidal marshes and mudflats along the embankments. The lower estuary is composed by extended sand banks along the axis forming well defined flood and ebb channels with an artificial navigation channel about 20 m deep. The mean average yearly combined discharge is about 100 m^3 s^{-1} and the mean tidal prism is about 10^9 m^3. Tides are semi-diurnal with mean tipical amplitudes of 2 m and extreme amplitude of 4 m. The estuary can be considered well-mixed to partially-mixed. The upstream limit of the mean position of the salinity intrusion is located at about 160 km from Vlissingen. The pattern of sediment distribution (Looff[1,2]) with detailed information on the composition of the sediments, percentage of sand, silt, organic content, calcium carbonate, and values of the median size of particles, show a patched distribution along the estuary. The strong variability of mineralogic and granulometric composition of the bottom sediments should reflect a distinct behaviour on sediment dynamics, being the turbidity maximum associated with the mobile stock of fine bed sediments. As in most partially mixed and well-mixed estuaries, a turbidity maximum-fluid mud system can be observed in the low salinity reaches (Antwerpen area) and migrates longitudinally in the estuary in response to changing tidal range and river flow. The turbidity zone is conditioned by a long residence time between 1-3 months in the brackish water zone which extends over 100km (Wollast[3]). This implies a high rate of accumulation of pollutants and significant modifications of the chemically active substances, with an impact on microbiological (Fisher[4]) and on biological processes at higher trophic levels (zooplankton, hyperbenthos, macrobenthos and meiobenthos) in the estuary (Simenstad et al[5]).

3 Numerical Calculation of Hydrodynamics and Sediment Transport

The sediment transport mechanisms in an estuary are mainly driven by tidal dynamics and the correspondent energy levels. Hydrodynamics controls the exchanges between the bottom and the water column as well as the horizontal

transport. Following the primary works of Einstein[6] and his collaborators, a large number of mathematical models have been developed (Ariathurai & Krone[7]; Hayter & Mehta[8]; Sheng[9]; O´Connor & Nicholson[10]; Van Rijn[11]; Mulder & Udink[12]; Teisson[13]; Cancino & Neves[14,15]; Li et al[16]). The basic differences between the various models arise from the number of dimensions considered, the numerical technique adopted and the complexity of the description of bed evolution. Nowadays numerical models are currently used for research and engineering purposes.

The hydrodynamic model used (briefly described in Appendix A) is a fully 3D-baroclinic model.It considers the hydrostatic and Boussinesq approximations, uses the vertical double sigma coordinate with a staggered grid and a semi-implicit two-time level scheme (Santos & Neves[17]; Santos[18]). The model solves the momentum and continuity equations, two transport equations for salt and temperature and an equation of state to include the baroclinic effects. For the baroclinic simulation of tidal flow and sediment transport a 600 m grid spacing, 6 vertical layers and a 30 s time step have been adopted. As boundary conditions the 17 main tidal constituents were specified at the open sea and the river discharge at the upstream end. Constant values of 30 psu and 0 psu (12^0 C and 14^0 C) respectively, were imposed at the sea and river boundaries.

The simulation of cohesive sediment transport processes is performed solving the 3D-advection-diffusion equation (Appendix A, eqn. 8), in the same sigma coordinate grid used by the hydrodynamic model (Cancino & Neves[15,16]). Considering a simple sigma coordinate the thickness of each layer is smaller in shallower areas. A double sigma coordinate (Santos[18]) dividing the vertical domain into two sub-domains by a horizontal plane will overcome the above mentioned restrictions. A direct consequence of confining the intertidal zones to the upper sub-domain is the increase of the time step used in numerical calculations. In cases of strong vertical density gradients this can also increase the accurancy of the numerical model (Dellersnijder & Beckers[19]). As open boundary conditions constant values of 0.05 gl^{-1} and 0.5 g l^{-1} were imposed respectively at the sea and river boundaries. A spatial distribution of dry density of bed sediments has been imposed along the estuary conditioning the threshold of erosion of the bed particles.The mass exchange with the bottom is accounted for by the erosion and deposition fluxes considered as a source/sink term for the layer closer to the bottom. Erosion occurs (eqn. 9) when the ambient shear stress exceeds the threshold of erosion of the bed particles (eqn. 10). This relation is a great simplification of reality, since the erodibility of a cohesive bed is a function of its cohesive nature depending also, in a poorly understood way, on the geochemistry, clay mineralogy and microbiology. The exchange of sediment particles between the layers of the model is a function of vertical diffusion, sediment settling velocity and vertical flow velocity. Relation (11) considers the effect of flocculation in differential settling. The deposition algorithm is based on the approach proposed by Krone [20] and later on modified by Odd & Owen[21]. No deposition occurs when the bottom shear stress is larger than a critical value for deposition. Otherwise the deposition rate is computed from the concentration of sediments and settling velocity at the water-bottom interface. Critical shear stress for deposition is assumed a constant value of 0.2 kg m^{-1} s^{-2} based on tidal experiments with natural mud from the Western Scheldt (Winterwerp[22]).

4 Results and Discussion

Results of the hydrodynamic and sediment transport model were validated using data collected in a cruise on the 27th-28th April 1994. The results of the

hydrodynamic model have been validated comparing calculated tidal levels with measurements in different points along the estuary. Since the mixing of fresh and salty water in the upper reaches of the estuary may produce density currents of the same order of magnitude as the residual barotropic currents the importance of these baroclinic effects were investigated.

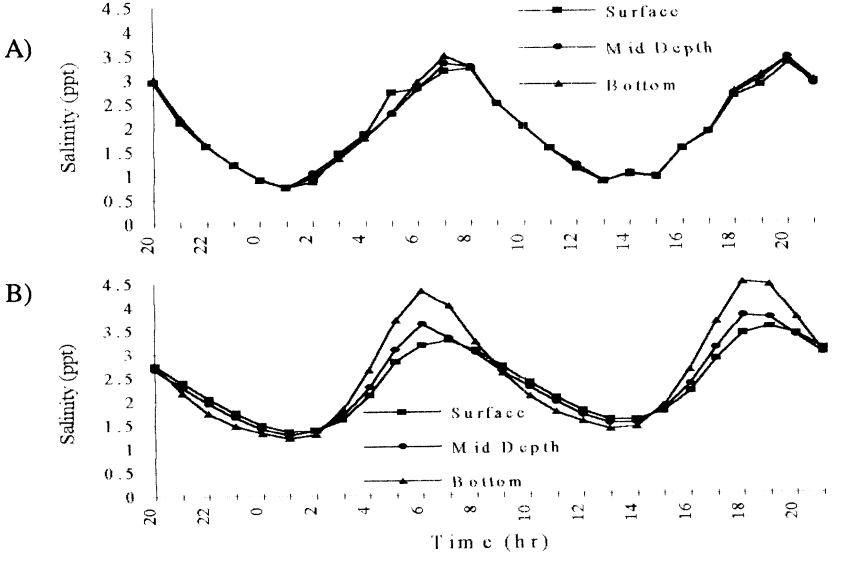

Figure 2: Comparison between the time variation of field salinity data (A) and model results (B) at the surface, mid depth and bottom for a 24 hr period for a station located in upper part of the estuary (27-28/04/94).

A comparison between the spatial distribution of salinity data and model results at the surface, mid depth and bottom for a station located in the upper part of the estuary (at 20 km from Bath) is presented in Figure 2. Model results (Fig. 2B) show a consistent pattern of salt behaviour through each tidal cycle. Higher salinity values were obtained during high water (at 7 and 20hrs), and lower values during low water (at 0 and 14hrs). Both figures show that during flood, stratification is much larger than during ebb. A significant change in the vertical profile is reached during ebb. During this period the tidal circulation leads to strong vertical shear and advection of fresher upper-estuary water over much slower saline water near the bed. Calculated 24hr time-series of velocity and salinity near the surface, at mid depth and near the bottom at a station in the lower part of the estuary (near Vlissingen) is shown in Figure 3. Maximum salinity values are reached at HW (which occurs approximately at 3:30 and 16hrs) and then fall rapidly before low water (which occurs aproximately at 10 and 22hrs). Velocity is higher at the surface, as expected, but it reaches twice the intensity during ebb at mid depth than at the surface. This occurrence seems to be associated to the bottom topography variation, to the local reduction of the width and to density effects. The simulation of cohesive sediment transport was performed accounting for the baroclinic effects of density currents. The calculated density current show an intensity two order of magnitute lower than the residual barotropic currents. Calculated settling velocity indicates that the range of intensity variation is between 0.5 mms^{-1} and 1.9 mms^{-1}. These values are in the

same range of the intensities obtained in laboratorial experiments with natural sediment suspensions collected during the campaign (unpublished data).

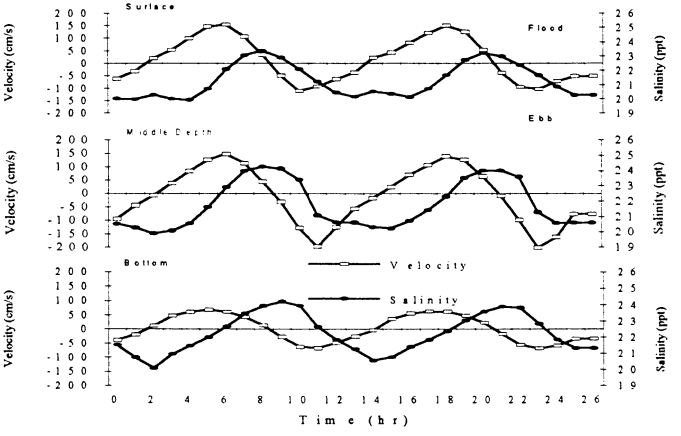

Figure 3: Calculated salinity and velocity near the surface, mid depth and bottom in Vlissingen the lower part of the estuary for a 24 hr period (27-28/04/94).

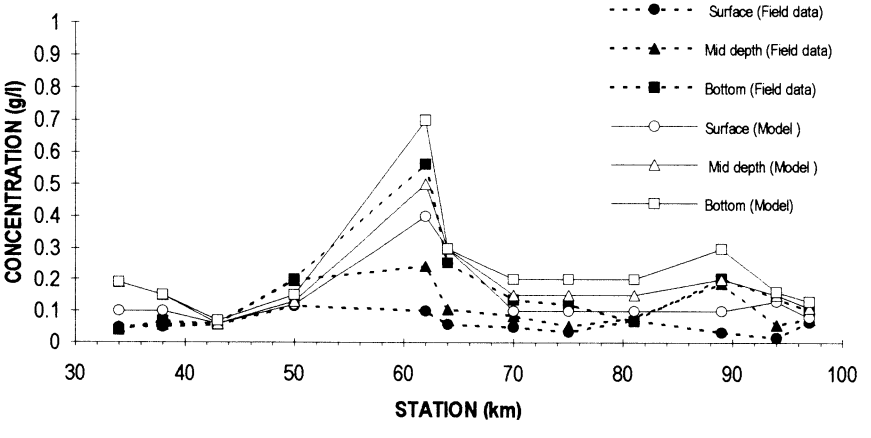

Figure 4: Comparison between calculated (solid lines) and observed (dashed lines) suspended sediment concentration (gl^{-1}) along a longitudinal transect during a 24 hr period (27-28/04/94). Distance (in km) measured upstream from Vlissingen.

A comparison of calculated and observed suspended sediment concentration along a longitudinal transect (from Hansweert till Temse, respectivelly 35, 98 km from Vlissingen) during a 24 hr period (Fig.4) show that the results in the main lower estuary are in better agreement with data than in the narrow upper estuary. It can be seen that the concentration near Zandvliev (62 km) is too much high. These measurements were taken during ebb maximum velocity period. Since erosion occurs mainly during this period and the deviation is larger near the surface, the obtained results suggest that in these area the vertical turbulent diffusivity should be decreased. Results at Rupelmonde (89 km) are refered to the period of maximum flood. The increase of the concentration in the model is

smaller than data values which suggest that ressuspension is also stronger in the nature. Nevertheless the available field data is not sufficient to fully support these conclusions.

Concluding Remarks

Results of 3-D baroclinic hydrodynamic and cohesive sediment transport model applied to the Western Scheldt estuary have been presented. The hydrodynamic simulation are in good agreement with the field data and provide an insight into the effetcs of stratification and its ebb-flood asymmetry. Since calculated density current show an intensity two order of magnitute lower than the residual barotropic currents the density effects on sediment transport are, on average, of less importance. The turbidity maximum zone should be associate directly with the geometry of the estuary, the advective transport and ressuspension processes. At the lower part of the estuary the sediment results are in considerable good agreement with the field data. In the upper reaches, the narrow part of the estuary, a different parametrization should be considered since the strong variability of bottom sediments reflect a distinct behaviour on sediment dynamics.

Appendix A

The momentum and continuity equations in cartesian coordinates are:

$$\frac{\partial u}{\partial t}+\frac{\partial (uu)}{\partial x}+\frac{\partial (uv)}{\partial y}+\frac{\partial (uw)}{\partial z}-fv+\frac{1}{r}\frac{\partial p}{\partial x}-\frac{1}{r}\left(\frac{\partial \tau_{xx}}{\partial x}+\frac{\partial \tau_{yx}}{\partial y}+\frac{\partial \tau_{zx}}{\partial z}\right)=0 \qquad (1)$$

$$\frac{\partial v}{\partial t}+\frac{\partial (vu)}{\partial x}+\frac{\partial (vv)}{\partial y}+\frac{\partial (vw)}{\partial z}+fu+\frac{1}{r}\frac{\partial p}{\partial y}-\frac{1}{r}\left(\frac{\partial \tau_{xy}}{\partial x}+\frac{\partial \tau_{yy}}{\partial y}+\frac{\partial \tau_{zy}}{\partial z}\right)=0 \qquad (2)$$

$$\frac{\partial p}{\partial z}+\rho g=0 \qquad \frac{\partial \xi}{\partial t}=-\int_{-h}^{\xi}\frac{\partial u}{\partial x}dz-\int_{-h}^{\xi}\frac{\partial v}{\partial y}dz \qquad (3,4)$$

where t is time, u, v, w are velocity components in x, y, z directions, f is Coriolis parameter, p pressure, ρ water density; τ shear stress, g acceleration of gravity, and ξ elevation of water surface.

As boundary condition at the bottom, the friction shear stress is imposed:

$$\tau=\xi c_d|\overline{u}_+|\overline{u}_+ \qquad c_d=k^2\left(\ln\frac{z_+}{z_\phi}\right)^2 \qquad (5,6)$$

where u_+ is horizontal velocity vector in x,y direction at some distance z_+ above the bottom, c_d is bottom drag coefficient, k von Karman constant and z_+ is physical roughness height.

The governing transport equations can be written as:

$$\frac{\partial S}{\partial t}+\frac{\partial uS}{\partial x}+\frac{\partial vS}{\partial y}+\frac{\partial wS}{\partial z}=\frac{\partial}{\partial x}\left(\varepsilon_{sx}\frac{\partial S}{\partial x}\right)+\frac{\partial}{\partial y}\left(\varepsilon_{sy}\frac{\partial S}{\partial y}\right)+\frac{\partial}{\partial z}\left(\varepsilon_{sz}\frac{\partial S}{\partial z}\right) \qquad (7a)$$

$$\frac{\partial T}{\partial t}+\frac{\partial uT}{\partial x}+\frac{\partial vT}{\partial y}+\frac{\partial wT}{\partial z}=\frac{\partial}{\partial x}\left(\varepsilon_{tx}\frac{\partial T}{\partial x}\right)+\frac{\partial}{\partial y}\left(\varepsilon_{ty}\frac{\partial T}{\partial y}\right)+\frac{\partial}{\partial z}\left(\varepsilon_{tz}\frac{\partial T}{\partial z}\right) \qquad (7b)$$

$$\frac{\partial C}{\partial t}+\frac{\partial uC}{\partial x}+\frac{\partial vC}{\partial y}+\frac{\partial (w+W_S)C}{\partial z}=\frac{\partial}{\partial x}\left(\varepsilon_x\frac{\partial C}{\partial x}\right)+\frac{\partial}{\partial y}\left(\varepsilon_y\frac{\partial C}{\partial y}\right)+\frac{\partial}{\partial z}\left(\varepsilon_z\frac{\partial C}{\partial z}\right) \qquad (8)$$

where S,T,C ,are the salt, temperature and suspended sediment concentration, t is time, x,y are the horizontal coordinates, z is the vertical coordinate, ε_x, ε_y, ε_z are salinity, heat and sediment mass diffusion coefficients, W_S the sediment fall velocity and u, v, w the flow velocity components in x, y, z directions.

The sediment erosion algorithm is based on the classical approach of Partheniades[23].

$$dM_E / dt = E(\tau / \tau_E - 1.0) \qquad : \tau > \tau_E \tag{9a}$$

$$dM_E / dt = 0 \qquad : \tau \leq \tau_E \tag{9b}$$

where the left hand sides of Eqs. 9a and 9b are the erosion fluxes; τ is bed shear stress ; τ_E is critical shear stress for erosion and E is the erosion constant (in kg $m^{-2}s^{-1}$). Critical shear stress for erosion is calculated as a function of the dry density of bed sediments based on the formulations proposed by Delo[24]:

$$\tau_E = A_1(\rho_d)^{E_1} \tag{10}$$

where τ_E is critical erosive stress (in N m^{-2}); ρ_d is dry density of bed sediments (in kg m^{-3}) and represents the ratio of dry mud mass and wet mud volume; A_1=0.0012 m^2 s^{-2}, E_1=1.2 and are coefficients depending on mud type.

Sediment settling velocity depends on flocculation processes and is calculated as a function of the concentration (Dyer[25]):

$$W_S = K_1 C^m \qquad : C \leq C_{HS} \tag{11a}$$

$$W_S = W_0(1.0 - C)^{m_1} \qquad : C > C_{HS} \tag{11b}$$

where W_S is sediment particles fall velocity (in m s^{-1}); W_0 is fall velocity of a single particle (m s^{-1}); C_{HS} is sediment concentration above which hindered settling occurs (kg m^{-3}); the constant of proportionality K_1=6.0 x 10^{-3} (kg m^{-4} s) depends on the mineralogy of the muds; exponents m and m_1 depend on particle size and shape with m=1.0; m_1=4.65 for small particles, m_1=2.32 and for large particles (Dyer[25]).

ACKNOWLEDGMENT

Most of this work was undertaken as a part of the project MATURE (Biogeochemistry of the MAximum TURbidity zone in Estuaries)/ CEC/ Environ.

REFERENCES

1. Looff, D. Kaartering van de Bobemsamenstelling van Het Oostelijk Gedeelte van de Westerschelde. Methode en Resultaten. *Rijkswaterstaat*, Rep. WWKZ nr. 78.V013, 10, 1978.

2. Looff, D. Kaartering van de Bobemsamenstelling van Het Westelijk Gedeelte van de Westerschelde. Methode en Resultaten. *Rijkswaterstaat*, Rep. WWKZ nr. 80.V009, 9, 1980.

3. Wollast, R. The Scheldt Estuary. In: W. Salomon, B.L. Bayne, E.K. Duursma and U. Forstner, Ed., *Pollution of the North Sea. An Assessment*. Springer-Verlag, p. 183-193, 1986.

4. Fisher, T.R., Harding, L.W. Jr., Stanley, D.W. & Ward, L.G. Phytoplankton, Nutrients, and Turbidity in the Chesapeake, Delaware, and Hudson Estuaries. *Estuar. Coast. Shelf Sci.* 27: 61-93, 1988.

5. Simenstad, C.A., Small, L.F. & McIntire, C.D. Consumption Processes and Food Web

Structure in the Columbia River Estaury . *Prog. ceanog.*, 25: 271-297, 1990.

6. Einstein, H. A. The Bedload Function for Sediment Transportation in Open Channel Flows. *Soil Cons. Serv. U. S. Dept. Agric. Tech. Bull.*, No. 1026, 78 pp, 1950.

7. Aariathurai, R. & R.B. Krone. Finite Element Model for Cohesive Sediment Transport. *J. Hydr. Div.*, ASCE, Vol. 102, No.HY3, p. 323-338, 1976.

8. Hayter, E.J. & Mehta, A.J. Modelling Cohesive Sediment Transport in Estuarine Waters. *Appl. Math. Moddeling*, 10: 294-303, 1986.

9. Sheng, Y.P. Modelling Bottom Boundary Layer and Cohesive Sediment Dynamics in Estuarine and Coastal Waters. In: A. J. Mehta, Ed., *Estuarine Cohesive Sediment Dynamics*, Springer, Berlin, 14: 360-400, 1986.

10. O'Connor, B.A. & Nicholson, J.A. Three-Dimensional Model of Suspended Particulate Sediment Transport. *Coastal Eng.* 12: 157-174, 1988.

11. Van Rijn, L.C. State of the Art in Sediment Transport Modeling. In: Sam S. Y. Wang, Ed., *Sediment Transport Modeling*, ASCE, p. 13-32, 1989.

12. Mulder, H.P.J. & Udink, C. Modelling of Cohesive Sediment Transport. A case study: The Western Scheldt Estuary. *Proceedings of the 22nd Intern. Conf. on Coastal Eng. American Society of Civil Engineers,* New York, p. 3012-3023, 1991.

13. Teisson, C. Cohesive Suspended Sediment Transport: Feasibility and Limitations of Numerical Modelling, *J. Hyd. Res.*, 29 (6), 755-769, 1991.

14. Cancino, L. & Neves, R. Numerical Modelling of Three-Dimensional Cohesive Sediment Transport in an Estuarine Environment. *World Scientific Publishing*,107-121, 1994a.

15. Cancino, L. and Neves, R. 3D-Numerical Modelling of Cohesive Suspended Sediment in the Western Scheldt Estuary (The Netherlands). *Netherlands Journal of Aquatic Ecology*, 28 (3-4), 337-345, 1994b.

16. Li, Z.H., Nguyen, K.D., Brun-Cottan, J.C. & Martin, J.M. Numerical Simulation of the Turbidity Maximum Transport in the Gironde Estuary (France), *Oceanologica Acta*, 1994.

17. Santos, A.J. & Neves, R. Radiactive Artificial Boundaries in Ocean Barotropic Models. *Proceedings of 2nd Int. Conf. on Comp. Modelling in Ocean Eng.* , Barcelona, 373-383, 1991.

18. Santos, A.J. *Modelo 3-D para Escoamentos de Superfície Livre*. Thesis submited for the degree of Doctor of Philosophy, I.S.T., Portugal, 1995.

19. Delleersnijder, E. & Beckers, J.-M. On the Use of the sigma-coordinate System in Regions of Large Bathymetric Variations. *Journal of Marine Systems*, 3, 381-390, 1992.

20. Krone, R.B. Flume Studies of the Transport in Estuarine Shoaling Processes. Hydr. Eng. Lab., Univ. of Berkeley, California, USA, 110 pp, 1962.

21. Odd, N.V.M. & Owen, M.W. A Two-Layer Model of Mud Transport in the Thames Estuary. Proceedings, *Institution of Civil Engineers*, London, p. 195-202, 1972.

22. Winterwerp, J.C., Cornelisse, J.M., & Kuijper C. The Behaviour of Mud from the Western Scheldt Under Tidal Conditions. *Delft Hydraulics*, The Netherlands, Rep. z161-37/HW/paper1.wm, 14 pp, 1991.

23. Partheniades, E. Erosion and Deposition of Cohesive Soils. *Journal of the Hydr. Div.*, ASCE, vol. 91, No. HY1: 105-139, 1965.

24. Delo, E.A. Estuarine Muds Manual. Report No. SR 164, *Hydraulics Research,* Wallingford, UK, 64 pp, 1988.

25. Dyer, K.R. Coastal and Estuarine Sediment Dynamics. *Wiley-Interscience*, New York,1986.